Electrolyte gated oxide pseudodiode for inhibitory synapse applications

Fu, Yang Ming; Wan, Chang Jin; Yu, Fei; Xiao, Hui; Tao, Jian; Guo, Yan Bo; Gao, Wan Tian; Zhu, Li Qiang

2018

Fu, Y. M., Wan, C. J., Yu, F., Xiao, H., Tao, J., Guo, Y. B., . . . Zhu, L. Q. (2018). Electrolyte gated oxide pseudodiode for inhibitory synapse applications. Advanced Electronic Materials, 4(11), 1800371-. doi:10.1002/aelm.201800371

https://hdl.handle.net/10356/90154

https://doi.org/10.1002/aelm.201800371

Advanced Electronic Materials

Electrolyte Gated Oxide Pseudo-Diode for Inhibitory Synapse Applications

--Manuscript Draft--

Manuscript Number:	aelm.201800371R1
Full Title:	Electrolyte Gated Oxide Pseudo-Diode for Inhibitory Synapse Applications
Article Type:	Full Paper
Section/Category:	
Keywords:	Electric-double-layer transistors; Pseudo-diode; Neuromorphic systems; Low power dissipation.
Corresponding Author:	Li Qiang Zhu Ningbo Institute of Materials Technology and Engineering Chinese Academy of Sciences Ningbo, Zhejiang CHINA
Corresponding Author Secondary Information:	
Corresponding Author's Institution:	Ningbo Institute of Materials Technology and Engineering Chinese Academy of Sciences
Corresponding Author's Secondary Institution:	
First Author:	Yang Ming Fu
First Author Secondary Information:	
Order of Authors:	Yang Ming Fu
	Chang Jin Wan
	Fei Yu
	Hui Xiao
	Jian Tao
	Yan Bo Guo
	Wan Tian Gao
	Li Qiang Zhu
Order of Authors Secondary Information:	
Abstract:	Recently, synaptic electronics are attracting increasing attentions in neuromorphic engineering. Here, inhibitory synapses are proposed based on nanogranular phosphorous silicate glass gated indium tin oxide transistors operated in pseudo-diode mode. Activity dependent inhibitory synaptic behaviors are mimicked on the proposed pseudo-diode, including paired pulse depression and depression adaptation behaviors. Interestingly, the proposed inhibitory synapse demonstrates low power dissipation as low as ~16fJ for triggering a post-synaptic current with high signal to noise ratio of ~2.2. Moreover, the inhibitory synapse demonstrates zero resting power dissipation. The proposed pseudo-diode based inhibitory artificial synapses may find potential applications in neuromorphic platforms.
Additional Information:	
Question	**Response**
Please submit a plain text version of your cover letter here. Please note, if you are submitting a	Dear Editor: Could you please find our attached file titled “Electrolyte Gated Oxide Pseudo-Diode for Inhibitory Synapse Applications” submitted to Advanced Electronic Materials. We have reply to the reviewer’s comments point-by-point. Some new data have been

revision of your manuscript, there is an opportunity for you to provide your responses to the reviewers later; please do not add them to the cover letter.	provided in the revised manuscript. We hope that our manuscript would be suitable for publication in Advanced Electronic Materials. Thanks With my best wishes Sincerely yours: Li Qiang ZHU
Do you or any of your co-authors have a conflict of interest to declare?	No. The authors declare no conflict of interest.

DOI: 10.1002/ ((please add manuscript number))
Article type: Full Paper

Electrolyte Gated Oxide Pseudo-Diode for Inhibitory Synapse Applications

Yang Ming Fu, Dr. Chang Jin Wan, Fei Yu, Hui Xiao, Jian Tao, Yan Bo Guo, Wan Tian Gao, Prof. Li Qiang Zhu *

Yang Ming Fu, Fei Yu, Hui Xiao, Jian Tao, Yan Bo Guo, Wan Tian Gao, Prof. Li Qiang Zhu
Key Laboratory of Graphene Technologies and Applications of Zhejiang Province, Ningbo Institute of Materials Technology and Engineering, Chinese Academy of Sciences, Ningbo 315201, Zhejiang, People's Republic of China and University of Chinese Academy of Sciences, Beijing 100049, Peoples Republic of China
E-mail: lqzhu@nimte.ac.cn

Dr. Chang Jin Wan
School of Materials Science and Engineering, Nanyang Technological University, 50 Nanyang Avenue, 639798, Singapore

Keywords:
Electric-double-layer transistors, Pseudo-diode, Neuromorphic systems, Low power dissipation.

Abstract:

Recently, synaptic electronics are attracting increasing attentions in neuromorphic engineering. Here, inhibitory synapses are proposed based on nanogranular phosphorous silicate glass gated indium tin oxide transistors operated in pseudo-diode mode. Activity dependent inhibitory synaptic behaviors are mimicked on the proposed pseudo-diode, including paired pulse depression and depression adaptation behaviors. Interestingly, the proposed inhibitory synapse demonstrates low power dissipation as low as ~16fJ for

triggering a post-synaptic current with high signal to noise ratio of ~2.2. Moreover, the inhibitory synapse demonstrates zero resting power dissipation. The proposed pseudo-diode based inhibitory artificial synapses may find potential applications in neuromorphic platforms.

1. Introduction

Brain-inspired neuromorphic engineering is becoming a hot topic in the field of information technology [1]. Conventionally, neuromorphic engineering is based on von Neumann architecture where the processor and the memory are physically separated. However, it is becoming increasingly inefficient when it meets complicated computation due to the limitations of parallel computation and high power dissipation. In nervous system, a synapse connects two neurons, underlining signal transmitting and information processing function [2]. Thus, realization of synaptic functions on solid state electronic devices would be of great significances for neuromorphic platforms. Recently, solid state electronic devices were designed for neuromorphic device applications, including memristors [3, 4], new-conceptual transistors [5, 6], spin-orbit torque devices [7], spintronic oscillators[8], etc. Such new-conceptual electronic synapses demonstrate great potentials in constructing neuromorphic platforms. Electrostatic modulating through ion gating enables realization of new conceptual devices with functions including superconductivity, ferromagnetism and Mott transition [9, 10]. With inherent properties and unique ion gating behaviors, ionic-liquid and ionic-gel electrolyte gated transistors (EGTs) have been creatively proposed for synaptic electronic applications. Several synaptic responses were mimicked, including excitatory postsynaptic current, paired-pulse facilitation, synaptic filtering, spatio-temporal integration, etc [11-13]. Recently, we have also reported synaptic membrane potential responses on solid-state electrolyte gated oxide transistors [14]. In neural activities, depression behaviors are also important signal transmitting forms related to sensory adaptations [15, 16]. However, they are seldom mimicked on electrolyte gated oxide transistors. Additionally, high resting power dissipation was expected for previously reported synaptic transistors, which is a serious shortcoming for building neuromorphic networks [12]. Moreover, as an important parameter, signal to noise ratio (S/N) has not been considered in previously reported solid-state synapse devices. In this work, nanogranular phosphorous silicate glass (PSG) gated indium tin oxide (ITO) transistors were fabricated, demonstrating a pseudo-diode operation mode. The pseudo-diode was proposed for inhibitory artificial synapse applications, exhibiting activity dependent inhibitory synaptic behaviors. Interestingly, the proposed inhibitory synapse demonstrates high signal to noise (S/N) ratio and low power dissipation. Zero resting power dissipation is observed. The pseudo-diode based inhibitory synapse may find potential applications in neuromorphic platforms.

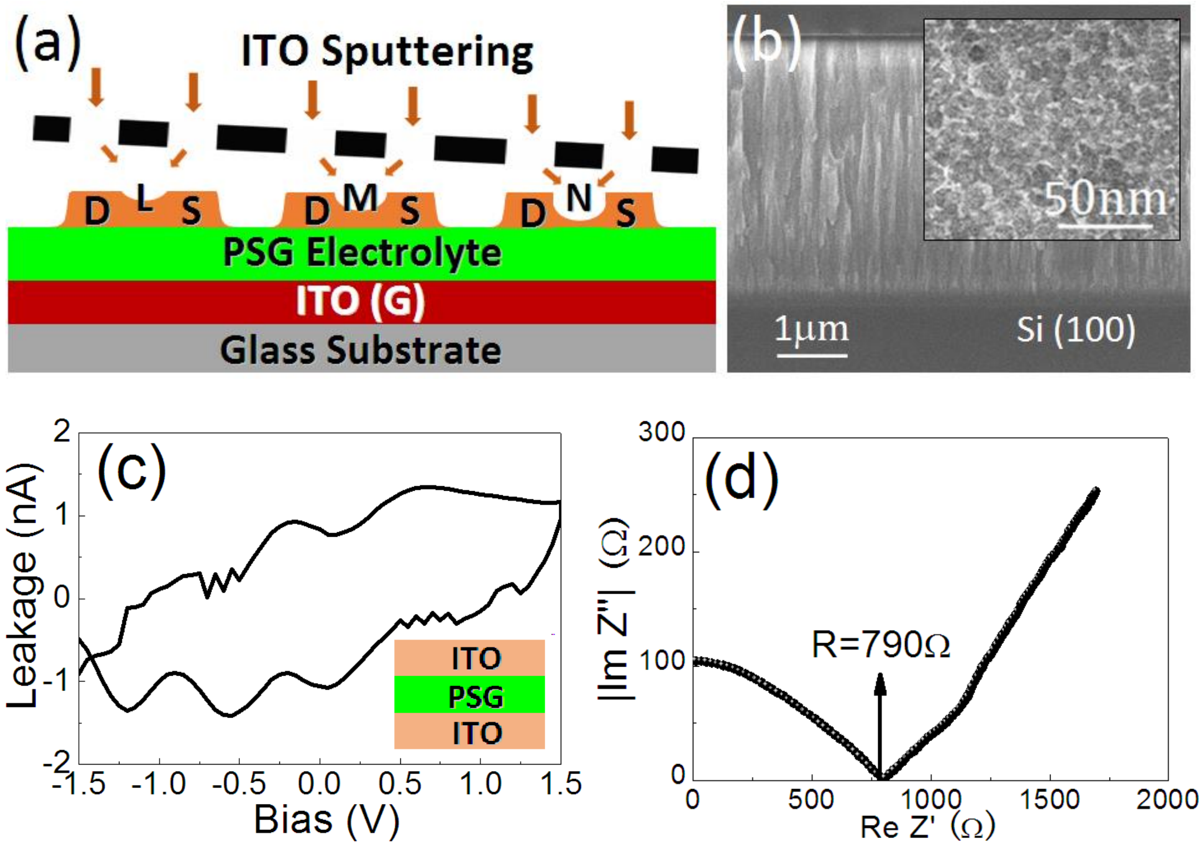

Figure 1 (a) Schematic diagram for obtaining ITO transistors. (b) Cross-sectional SEM image of nanogranular PSG film. Inset: TEM image of nanogranular PSG film deposited on Cu grid. (c) Leakage current for PSG film. Inset: ITO/PSG/ITO sandwiched testing structure. (d) Cole-

Cole plots of the impedance spectrum of the PSG film. Proton conductivity is estimated with a relation: $\sigma = D/(R-R_0)A$, where R_0 and A are ~30 Ω and 1.5×10^{-3} cm^2, respectively.

2. Results and Discussions

Figure 1(b) shows cross-sectional SEM image of the nanogranular PSG electrolyte film deposited on Si wafer. Thickness (D) is estimated to be ~4 μm. Inset in Figure 1(b) illustrates high-resolution TEM image of the nanogranular PSG film deposited on a Cu grid. The size of PSG nano-particles is in the order of 10 nm. The results indicate that there are nano-channels within the PSG electrolyte film. Figure 1(c) illustrates leakage current of PSG electrolyte in an ITO/PSG/ITO sandwich structure. The leak current is below 2 nA with the biases ranged between -1.5 V and 1.5 V. Proton conductivities of the PSG electrolyte were determined by using a Solartron 1260A impedance analyzer. Figure 1(d) illustrates Cole-Cole plots of the impedance spectrum. An impedance real value (R) of ~790 Ω is obtained with the impedance imaginary value equal to zero. Thus, proton conductivity (σ) is estimated to be ~3.5×10^{-4} S/cm.

Figure 2(a) illustrates frequency dependent specific capacitance of the PSG electrolyte film taken on an ITO/PSG/ITO sandwiched testing structure. An extremely high electric-double-layer (EDL) capacitance of ~5.2 μF/cm^2 is observed at 1Hz due to the accumulation of protons at PSG/ITO interface within the region of ~1 nm. Figure 2(b) shows transfer curves for transistors L, M and N measured at V_{ds} of 1.5V. There are no transistor performances for transistor L, indicating bad electrostatic modulation activities for thick ITO channel. While for transistors M and N, transistor performances are much better. For transistor M, current on/off ratio, subthreshold swing (SS) and mobility are estimated to be ~9.8×10^7, ~84 mV/decade and ~2.8 cm^2/Vs, respectively. While for transistor N, current on/off ratio, SS and mobility are estimated to be ~7.9×10^7, ~76 mV/decade and ~0.5 cm^2/Vs, respectively. In transistor operation mode, channel conductivities are modulated by biasing gate electrode.

With unique proton gating behaviors, channel conductance can also be modulated when the gate is grounded demonstrating pseudo-diode operating mode. Figure 2(c) shows IV curves for transistors L, M and N with bottom gate grounded. For drain bias at +1.5V, channel currents are estimated to be ~175μA, ~28μA and ~45nA for transistors L, M and N, respectively. While for drain bias at -1.5V, channel currents are estimated to be ~288μA, ~196μA and ~54μA for transistors L, M and N, respectively. Thus, the rectification ratios are estimated to be ~1.6, ~5.7 and ~1.2×10^3 for transistors L, M and N, respectively. The observations indicate the improved rectification behavior for decreased channel thickness. The behaviors can be explained as follows. When the pseudo-diode is positively biased, protons within the PSG film will accumulate at PSG/gate interface and PSG/source interface, which depletes the ITO channel, as schematically shown in the left-inset of Figure 2(c). When the pseudo-diode is negatively biased, protons will accumulate at PSG/channel interface, which results in the increased channel conductance, as schematically shown in the right-inset of Figure 2(c).

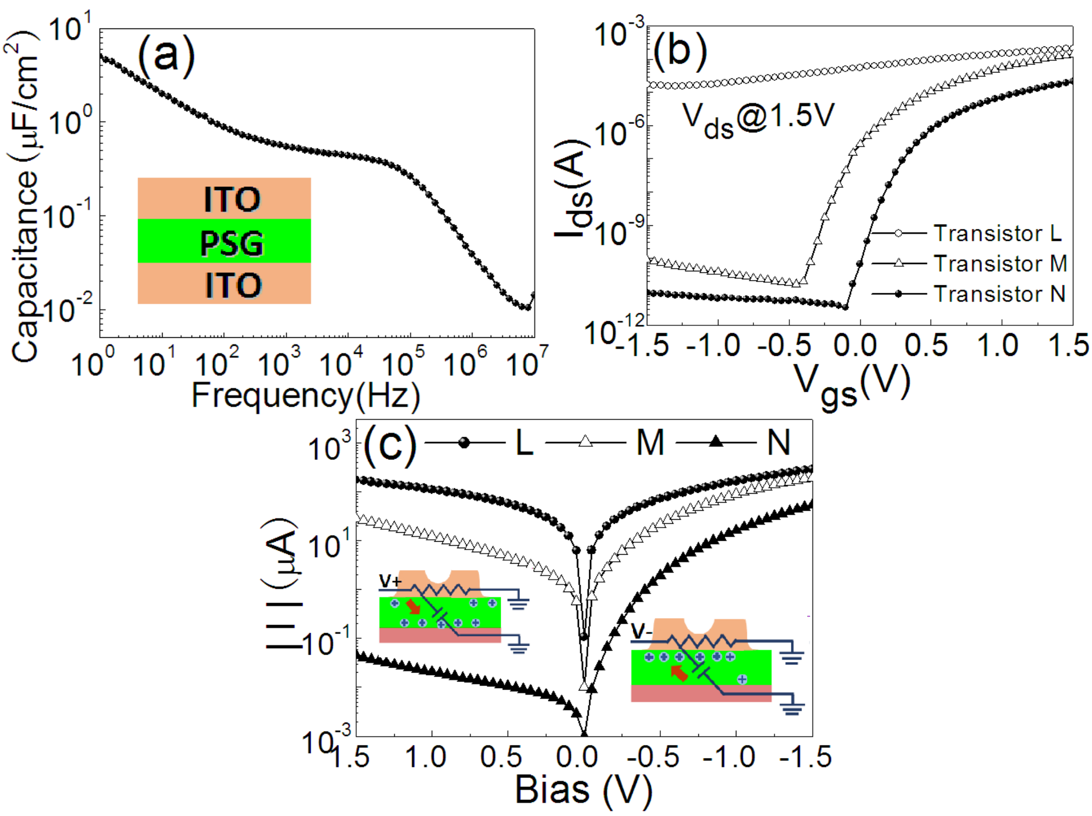

Figure 2 (a) Frequency dependent specific capacitance of nanogranular PSG film. Inset: ITO/PSG/ITO sandwiched testing structure. (b) Transfer curves of the ITO EDL transistors. (c) IV curves for transistors L, M and N operated at pseudo-diode mode.

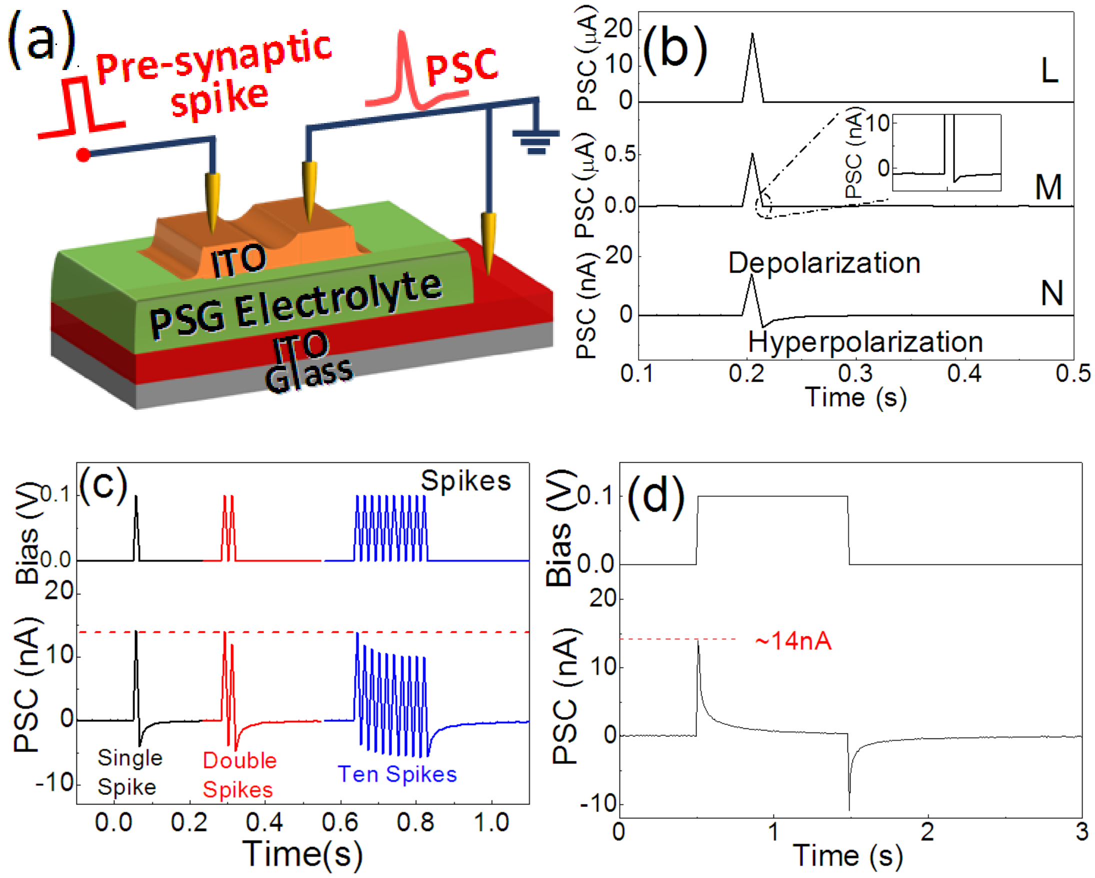

Figure 3 (a) Schematic diagram of inhibitory synapse based on electrolyte gated pseudo-diode (EGPD). (b) Transient currents of EGPDs triggered with a voltage spike of (0.1 V, 10 ms). (c) Transient currents of EGPD N triggered with multi-spikes of (0.1 V, 10 ms). (d) Transient currents of EGPD N triggered with a voltage spike of (0.1 V, 1 s).

In neural systems, synaptic fatigue, or short-term synaptic depression (STD), is thought to be a form of negative feedback in nervous systems. It is usually attributed to the depletion of the readily releasable vesicles.[17] This temporary reduction of synaptic connection is also an important form of signal modulation underlining brain functions [18]. In the nanogranular PSG electrolyte gated pseudo-diode (EGPD), a positive drain bias induces a decreased channel conductance. Thus, it is possible to mimic synaptic depression behaviors on the proposed EGPD. As schematically shown in **Figure 3**(a), a pre-synaptic spike is applied on the drain, while the channel current is deemed as post-synaptic current (PSC). Firstly, EGPDs L, M and N were triggered with a voltage spike of (0.1V, 10ms). Figure 3(b) illustrates the triggered transient currents. It is observed that the peak PSC currents are ~19µA, ~0.5µA and ~14nA for EGPDs L, M and N, respectively. When spike ends, the PSC turns back to zero for EGPD L. While for EGPD M, a negative peak current of ~-3nA is observed when the spike ends. The value is only ~0.6% of peak PSC value. Then, the current decays back to zero. While for EGPD N, the negative peak current is ~-4nA, which is ~29% of peak PSC value. The transient current hints the plasticity behaviors of the proposed EGPDs. The positive and negative PSCs can be deemed as depolarization and hyperpolarization behaviors in bio-synapse [19, 20]. We have obtained transient currents on EGPD N triggered by multi-spikes of (0.1 V, 10 ms) with interval time of 10 ms, as shown in Figure 3 (c). The first positive peak PSC currents are always ~14 nA. Figure 3 (d) illustrates transient current of EGPD N triggered with a voltage spike of (0.1V, 1 s). The positive peak PSC value is still ~14 nA. Thus, the first positive peak PSC value is related to intrinsic channel conductance. The negative PSC response is related to discharging process in PSG based electrolyte. When spike comes, proton will get accumulated at gate region and source region, which results in the decayed positive PSCs (Figure 3d). The operation mechanism is schematically shown in the left-inset of Figure 2(c). The process can be deemed as a charging behavior. When the spike ends, protons will diffuse back. Thus, a negative discharging current is triggered due to the increases in channel carrier density. Due to the slow migration of protons within the PSG electrolyte film, decayed discharging current is observed. Because the intrinsic channel conductance is very big for EGPD L, charging and discharging behaviors are less important for EGPD L.

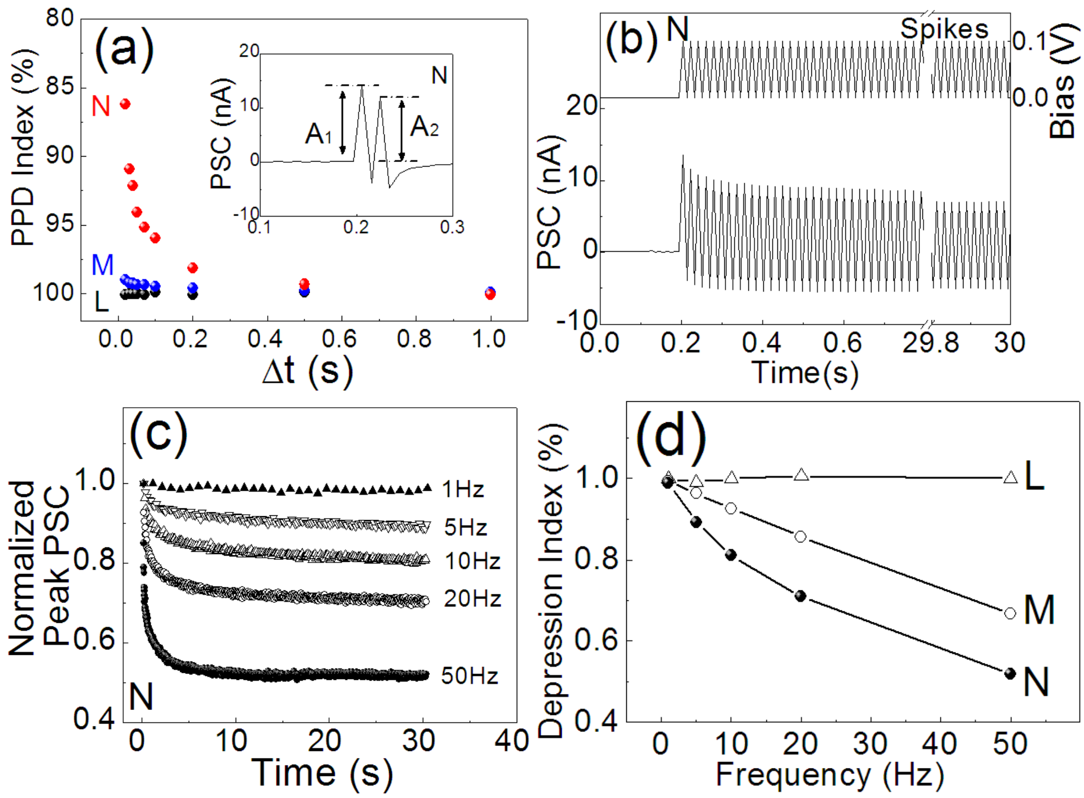

Figure 4 (a) PPD index (A2/A1×100%) as a function of interval time (Δt). Inset: PSC responses of EGPD N upon two subsequent pre-synaptic spikes of (0.1 V, 10 ms) with Δt of 20 ms. (b) PSC responses upon consecutive spikes (0.1 V, 10 ms) with Δt of 10 ms for EGPD N. (c) Normalized peak PSC values at different spike frequencies for EGPD N. (d) Depression index as a function of frequencies for EGPDs L, M and N.

In nervous system, paired-pulse depression (PPD) is one of the most commonly reported forms of short-term depression [21]. Here, the PPD response is also mimicked on the proposed EGPD based artificial synapses. Inset in **Figure 4**(a) shows PSC responses of EGPD N upon two subsequent pre-synaptic spikes of (0.1 V, 1 ms) with spike interval time (Δt) of 20 ms. The first peak PSC (A1) and the second peak PSC (A2) are ~14 nA and ~12 nA, respectively. The results indicate the depression behavior for EGPD N. The PPD behaviors are also attributed to unique protonic modulation effect. When the first spike comes, protons get accumulated at the PSG/gate and PSG/source interface. When the first spike ends, protons will migrate back to their equivalent positions. However, if the interval time between the first spike and the second spike is short enough, some protons will reside at the interface when the second spike comes. Thus, A2 is lower than A1. The depression behavior observed here is quite similar to that in bio-system [22]. Here, PPD index is defined as 100%×A2/A1. Figure 4(a) shows PPD index as a function of Δt. For EGPD L, the PPD index is always ~100 %. For EGPD M, PPD index increases slight from ~99 % to ~100 %. While for EGPD N, the PPD index increases from ~86 % to ~100 % with Δt increases from 20 ms to 1 s. It should be noted here that the charging behavior will degrade when the channel conductance is very high with thick channel layer. In this case, there are negligible proton accumulation at the PSG/gate interface and PSG/source interface. Thus, the depression behavior will get less importance. The results here indicate activity dependent synaptic depression behaviors for the proposed EGPD based synapse.

We have also applied consecutive spikes (0.1V, 10 ms) on the EGPD based inhibitory synapse. Figure 4(b) shows a typical PSC response upon consecutive spikes (0.1 V, 10 ms) with Δt of 20 ms for EGPD N. When the first spike comes, a peak PSC value of ~14 nA is observed. With the increased spike number, it decreases correspondingly. At last, the peak PSC value saturates at ~7 nA. The behaviors can be explained as follows. During the spike duration time, protons will be extracted and accumulate at the PSG/gate interface and PSG/source interface. While at the spike interval time, they will diffuse back to their initial equivalent position. Interestingly, some of the triggered protons will reside at the interface region depending on the spike interval time (Δt). Thus, more and more protons will accumulate at the interfaces with the increased spike numbers. When accumulation is balanced with diffusion back, the peak PSC tends to saturate. With the inherent properties for proton migration, the depression-stead phenomenon is duration time and interval time dependent. In another word, the depression-stead phenomenon is depended on the spike frequency. Figure 4 (c) shows normalized peak PSCs at different spike frequencies for EGPD

N. Here, the peak PSC values are normalized to the first peak PSC at each frequency. The saturated normalized peak PSC is defined as depression index. It is observed that the depression index decreases from ~0.98 to ~0.5 with the increased frequency from 1 Hz to 50 Hz. Interestingly, the depression-stead phenomena are also activity dependent for EGPD based artificial synapse. Figure 4 (d) illustrates the depression index as a function of frequency for EGPDs L, M and N. For EGPD L, there are no observable changes in the depression index because of the ignorable depression behaviors. For EGPD M, the depression index decreases from ~1 to ~0.67 with the increased frequency from 1 Hz to 50 Hz due to the increased temporal depression behaviors. While for EGPD N, the temporal depression behaviors get significant. Thus, the depression index decreases from ~0.98 to ~0.5. In nerve system, short term plasticity also endows biological synapse with the capability of signal calculation and decoding. [23] A series of consecutive spikes will lead to depression-stead phenomena due to the limited number of neurotransmitters in neurons. This depression-stead phenomena are regarded as one of the most efficient neural coding strategies.[24] Thus, the mimicked depression-stead phenomena endow the proposed EGPD based inhibitory synapse great potential.

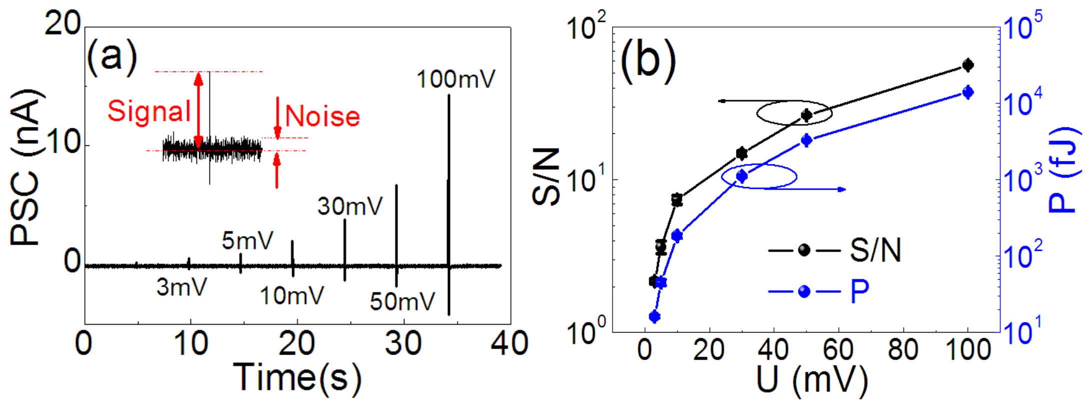

Figure 5 (a) PSC responses of EGPD based inhibitory synapse N on spikes with different spike amplitudes (U). The spike duration time (T) is 10 ms. Inset: Schematic diagram for obtaining S/N ratio. (b) Energy consumption (P) and signal to noise (S/N) ratio as a function of U.

For neuromorphic engineering applications, both low energy consumption (P) and high signal to noise ratio (S/N) are needed. **Figure 5** (a) illustrates PSC responses of EGPD based inhibitory synapse N on spikes with different spike amplitudes (U). The spike duration time (T) is 10 ms. The energy consumption (P) is estimated with a relation: P=Ipsc×U×T. Figure 5 (b) shows P and S/N as a function of U. With the decreased U values, both P and S/N values decrease. When U is 100 mV, P and S/N values are estimated to be ~14 pJ and ~56, respectively. When U is 3 mV, P is estimated to be only ~16 fJ. While the S/N value is still as large as 2.2. In terms of applications, S/N should be above a certain threshold value. When setting the threshold value at 2, S/N of 2.2 would be OK. In this case, the spike amplitude of 3 mV can be adopted. As comparison, the P value in biological synapse is ~10fJ/spike. [25, 26] And the spike amplitude in neural system is tens of mV. Thus, U value of 5 mV is preferred. At this U value, S/N ratio and P value are ~3.6 and ~45 fJ, respectively. Presently, the size of the EGPD based synapse is in the order of sub-1 mm. Intrinsically, PSG gated synaptic device could be scaled down to sub-100 nm. Thus, the energy consumption could decrease to sub-fJ level. Furthermore, resting power dissipation should be as low as possible for synaptic devices. In our previous reported oxide synaptic transistors, non-zero resting powers are always observed at resting state due to the constant V_{ds}. Here, no resting energy dissipation is observed for the pseudo-diode based inhibitory synapse due to the zero bias at resting state. As are interesting for neuromorphic platform applications.

3. Conclusions

In summary, pseudo-diode operation mode is reported on indium tin oxide (ITO) electric-double-layer transistor gated by nanogranular PSG based electrolyte, demonstrating activity dependent current rectification behaviors. The current rectification is related to the field-configurable proton fluxes within the electrolyte. The electrolyte gated pseudo-diode is proposed for inhibitory synapse applications, exhibiting activity dependent inhibitory synaptic behaviors including paired pulse depression and depression adaptation behavior. Furthermore, the pseudo-diode based inhibitory synapse demonstrating ultralow power dissipation. A low power dissipation as low as ~16 fJ is observed for triggering a post-synaptic current with high signal to noise ratio of ~2.2. Zero resting power dissipation is also observed. The proposed pseudo-diode based inhibitory synapse may find potential applications in neuromorphic platforms.

4. Experimental Section

Fabrication of indium tin oxide (ITO) transistors: Indium tin oxide (ITO) transistors were fabricated at room temperature. Firstly, nanogranular phosphorous silicate glass (PSG) films were deposited on ITO glass substrate by plasma enhanced chemical vapor deposition using SiH_4/PH_3 mixture and O_2 as reactive gases. Nanogranular PSG films were also deposited on polished Si wafer and Cu grid for receiving cross-sectional scanning electron microscopy (SEM) measurements and transmission electron microscopy (TEM) measurements. Then, patterned ITO films were deposited on the PSG films by sputtering an ITO ceramic target (In_2O_3: SnO_2=90 wt %: 10 wt %). A gradient metal mask is used, as schematically shown in Figure 1(a). ITO channels can be formed between source and drain electrodes due to reflection of sputtered ITO nanoparticles at mask edge. The gradient mask enables to obtain ITO channels with different thicknesses of ~62 nm, ~44 nm and ~25 nm. Correspondingly, the ITO transistors are denoted as L, M and N, respectively. Channel length and channel width are 80 μm and 1 mm, respectively.

Electrical Measurements: Proton conductivity and specific capacitance of the nanogranular PSG electrolytes were characterized by Solartron 1260A impedance analyzer. Electrical performances of ITO transistors and pseudo-diodes were characterized by Keithley 4200 SCS semiconductor parameter analyzer. All the measurements were carried out at room temperature with a relative humidity (RH) of ~55%.

Acknowledgements

This work was supported by Zhejiang Provincial Natural Science Foundation of China (LR18F040002), Ningbo Science and Technology Innovation Team (2016B10005), National Natural Science Foundation of China (11474293), Youth Innovation Promotion Association CAS (2014259), Key Research Program of Frontier Sciences, Chinese Academy of Sciences (QYZDB-SSW-JSC047) and CAS Interdisciplinary Innovation Team.

Received: ((will be filled in by the editorial staff))
Revised: ((will be filled in by the editorial staff))
Published online: ((will be filled in by the editorial staff))

References

[1] M. A. Zidan, J. P. Strachan, W. D. Lu, *Nat. Electron.*, **2018,** *1*, 22.

[2] N. Brunel, V. Hakim, M. J. Richardson, *Curr. Opin. Neurobio*. **2014**, *25*, 149.

[3] Z. Q. Wang, H. Y. Xu, X. H. Li, H. Yu, Y. C. Liu, X. J. Zhu, *Adv. Funct. Mater.*, **2012**, *22*, 2759

[4] J. Lee, W. D. Lu, *Adv. Mater.*, **2018**, *30*, 1702770.

[5] Q. X. Lai, L. Zhang, Z. Y. Li, W. F. Stickle, R. S. Williams, Y. Chen, *Adv. Mater.*, **2010**, *22*, 2448.

[6] F. Alibart, S. Pleutin, O. Bichler, C. Gamrat, T. Serrano-Gotarredona, B. Linares-Barranco, D. Vuillaume, *Adv. Funct. Mater*., **2012**, *22*, 609

[7] S. Nakhaie, J. M. Wofford, T. Schumann, U. Jahn, M. Ramsteiner, M. Hanke, J. M. J. Lopes, H. Riechert, *Appl. Phys. Lett*., **2015**, *106*, 213108.

[8] J. Torrejon, M. Riou, F. A. Araujo, S. Tsunegi, G. Khalsa, D. Querlioz, P. Bortolotti, V. Cros, K. Yakushiji, A. Fukushima, H. Kubota, S. Yuasa, M. D. Stiles, J. Grollier, *Nature*, **2017**, *547*, 428

[9] Y. Wang, J. Xiao, H. Zhu, Y. Li, Y. Alsaid, K. Y. Fong, Y. Zhou, S. Wang, W. Shi, Y. Wang, A. Zettl, E. J. Reed, X. Zhang, *Nature*, **2017**, *550*, 487.

[10] N. Lu, P. Zhang, Q. Zhang, R. Qiao, Q. He, H.-B. Li, Y. Wang, J. Guo, D. Zhang, Z. Duan, Z. Li, M. Wang, S. Yang, M. Yan, E. Arenholz, S. Zhou, W. Yang, L. Gu, C.-W. Nan, J. Wu, Y. Tokura, P. Yu, *Nature*, **2017**, *546*, 124.

[11] H. Tian, W. Mi, X.-F. Wang, H. Zhao, Q.-Y. Xie, C. Li, Y.-X. Li, Y. Yang, T.-L. Ren, *Nano Lett.*, **2015**, *15*, 8013.

[12] L. Q. Zhu, C. J. Wan, L. Q. Guo, Y. Shi, Q. Wan, *Nat. Commu.*, **2014**, *5*, 3158.

[13] P. Gkoupidenis, N. Schaefer, X. Strakosas, J. A. Fairfield, G. G. Malliaras, *Appl. Phys. Lett.*, **2015**, *107*, 263302.

[14] Y. M. Fu, C. J. Wan, L. Q. Zhu, H. Xiao, X. D. Chen, Q. Wan, *Adv. Biosys.*, **2018**, *2*, 1700198

[15] M. Hollins, F. Lorenz, D. Harper, *J. Neurosci.*, **2006**, *26*, 5582.

[16] D.P.-González, M. S. Malmierca, *Front. Integr. Neurosci.*, **2014**, *8*, 19.

[17] M. V. Tsodyks, H. Markram, *Proc. Natl. Acad. Sci.*, **1997**, *94*, 719.

[18] L. A. Grande, W. J. Spain, *Physiology.*, **2005**, *20*, 201.

[19] M. Hausser, A. Roth, *J. Neurosci.*, **1997**, *17*, 7606.

[20] A. J. Smith, S. Owens, I. D. Forsythe, *J. Physiol.*, **2000**, *529*, 681.

[21] D.V.Buonomano, W.Maass, *Nat. Rev. Neurosci.*, **2009**, *10*, 113.

[22] L.S.Leung, P.Peloquin, K.J.Canning, *Hippocampus*, **2008**, *18*, 1008.

[23] L. A. Grande, W. J. Spain, *Physiology*, **2005**, *20*, 201.

[24] A. L. Fairhall, G. D. Lewen, W. Bialek, R. R. R. Steveninck, *Nature*, **2001**, *412*, 787.

[25] W. Xu, S.-Y. Min, H. Hwang, T.-W. Lee, *Sci. Adv.*, **2016**, *2*, e1501326.

[26] D. Kuzum, S. Yu, H.-S. P. Wong, *Nanotechnology*, **2013**, *24*, 382001.

The table of contents entry:

Inhibitory synapses are proposed based on oxide electric-double-layer transistors operated in pseudo-diode mode due to unique interfacial protonic coupling. Activity dependent inhibitory synaptic behaviors are observed on the proposed pseudo-diode. The inhibitory synapse demonstrates low power dissipation as low as ~16 fJ with high signal to noise ratio of ~2.2. Moreover, the inhibitory synapse demonstrates zero resting power dissipation.

Keyword: Electric-double-layer transistors, Pseudo-diode, Neuromorphic systems, Low energy dissipation.

Title: Electrolyte Gated Oxide Pseudo-Diode for Inhibitory Synapse Applications

ToC figure: